

# Effect of V-III Molar Flow Ratios on InAs Nanowire Structure Formation at crystal Quality

Deepak Anandan<sup>1</sup>, Hua Lun Ko<sup>3</sup>, Ramesh Kumar Kakkerla<sup>1</sup>, Hung-Wei Yu<sup>1</sup>, Venkatesh Nagarajan<sup>1</sup>, Sankalp Kumar Singh<sup>1</sup>, Edward Yi Chang<sup>1,2,3</sup>

<sup>1</sup>Department of Materials Science and Engineering, National Chiao-Tung University  
1001 University Road, Hsinchu 30010, Taiwan R.O.C

<sup>2</sup>Department of Electronic Engineering, National Chiao-Tung University, Taiwan

<sup>3</sup>International College of Semiconductor Technology, National Chiao-Tung University, Taiwan  
Phone: +886936842470 E-mail: edc@mail.nctu.edu.tw

## Abstract

The effect of V-III molar flow scaling on crystal quality of selectively grown InAs nanowires on patterned Si (111) substrate was investigated by metal organic vapor phase epitaxy (MOCVD). It is found that high aspect ratio of InAs NW can be achieved for optimized V/III ratio of 264. While scaling down the total molar flow rate and by keeping constant V/III ratio of 264, we found WZ (wurtzite) dominant crystal structure for high molar flow whereas for low flow, NW exhibits polytype WZ/ZB (zincblende) crystal structure for every 3-5 monolayer. Electrical characteristics proves that WZ dominated NW exhibits 1.6 times lower resistivity than polytype NWs.

## 1. Introduction

In past decades, NW synthesis was done mostly by external catalyst assist method. Herein, the supersaturation of Au-III alloy temperature window is larger, thereby it is possible to synthesis WZ and ZB crystal structures within a same NW. However, Au behaves as an impurity in Si, which is incompatible with modern CMOS technology [1]. Selective area growth (SAG) method of vertical III-V NW is one of the promising method to overcome aforesaid problem. Unfortunately, SAG using MOCVD is always mixed up with WZ/ZB phase in a single NW [2]. In order to ease WZ/ZB mixture, here an effort was taken on effective molar flow rate scaling by keeping constant V/III ratio of 264. Hence, the high aspect ratio SAG was achieved with higher V/III ratio (264) as shown in fig. 1 (f). Transmission electron microscopy (TEM) analysis proves that higher molar flow synthesizes WZ dominated InAs NW, whereas lower flow ends up with equally mixed WZ/ZB crystal structure. Electrical characteristics show that WZ rich InAs NW exhibits 1.6 times lower resistivity than equally mixed WZ/ZB crystal structure.

## 2. Experiment

Synthesis of all SAG-InAs NWs were done by Veeco D180-MOCVD. Initially, 25-nm thick SiON was deposited on native oxide removed Si-(111) substrate by plasma enhanced chemical vapor deposition (PECVD). SiON/Si(111) was patterned using E-beam and wet etching (diluted BOE) process. The final diameter of opening of pattern was in the range of 150~180 nm. After loading the sample into main chamber, sample was annealed for 5 at 850 °C, then the temperature was reduced to 400 °C for Si-(111)B reconstruction in H<sub>2</sub> + arsine (AsH<sub>3</sub>) ambient. Finally, the

temperature was ramped to 540 °C and trimethylindium (TMIn) was injected into the chamber for NW growth, then it was switched off at the end. The samples were cooled under AsH<sub>3</sub> environment. Here, four set of experiments were conducted by fixing V/III=264. V<sub>1</sub>/III<sub>1</sub>=4.87×10<sup>-3</sup>/1.85×10<sup>-5</sup> (mole/min), V<sub>2</sub>/III<sub>2</sub>=2.44×10<sup>-3</sup>/9.23×10<sup>-6</sup>, V<sub>3</sub>/III<sub>3</sub>=1.62×10<sup>-3</sup>/6.15×10<sup>-6</sup> and V<sub>4</sub>/III<sub>4</sub>=0.812×10<sup>-3</sup>/3.08×10<sup>-6</sup>. The structural characteristics of the InAs NWs were observed by scanning electron microscopy (SEM, Hitachi SU-8010) and TEM (JEOL JEM-2010F), respectively. Raman spectra were recorded on as-grown sample to analyze structural information of NWs at room temperature by using 514.5-nm Ar<sup>+</sup> laser (Stellar-Pro 514/50, 514.5-nm). For resistivity measurement, p-type Si samples with a 500 nm SiO<sub>2</sub> (PECVD) insulating surface layer were prepared. Using photo lithography, Ni/Au (50/300 nm) metal pad deposition was done by E-gun and above that NWs were mechanically transferred. Prior to making electrical connectivity between NW and metal pad by platinum [3] using FIB, samples were subjected to HCL: H<sub>2</sub>O (1:10) etch for 30 s to remove native oxide on InAs surface. Fig. 3 (b) shows the final device with 2 μm length NW. A 2-probe configuration was used to measure electrical resistivity individual NW (totally 18 devices were made).

## 3. Results and Discussion

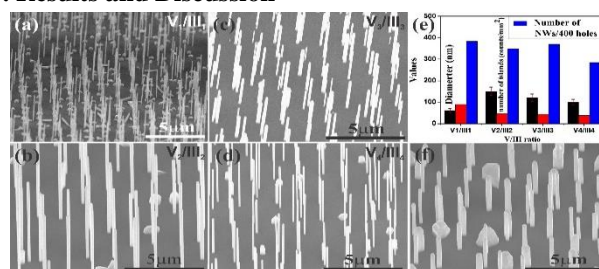


Fig. 1. (a) - (d) 45° tilted SEM images of SAG-InAs NWs for different molar flow by fixing constant V/III ratio 264. (e) Histogram representation of yield, diameter and island density for different molar flow. (f) SAG-InAs NW grown for V/III ratio of 88.

Fig. 1 (a) - (d) represents the SEM images of selectively grown InAs NWs arrays on Si-(111) substrate for different molar flow rate. It is observed that for higher flow rate, InAs NW follows selective area growth as well as random NW nucleation on passivated oxide surface. On reducing molar flow rate, a significant improvement in selectivity is observed. This is because, rich Indium (In) adatom diffuses into oxide pin holes and starts nucleation from the substrate [4]. As the

In flow rate decreases, the probability of In adatom migration to the nano hole is higher than the nucleation of NWs on oxide pin holes. On further reduction in molar flow rate, competition between adatoms inside the holes increasing, thereby, nucleating more than one NWs per hole [5]. Finally, at constant growth temperature with high molar flow, NW nucleates with larger diameter ( $140 \pm 10$  nm) than low molar flow ( $100 \pm 5$  nm). Also, NW growth yield reduces as molar flow decreases due to the evaporation of In adatom from the hole which is shown in histogram fig. 1 (e). By reducing the  $\text{AsH}_3$  flow ( $V/\text{III} = 88$ , fig. 1 (f)), the NW height is fairly low as compared to sample  $V_2/\text{III}_2$ .

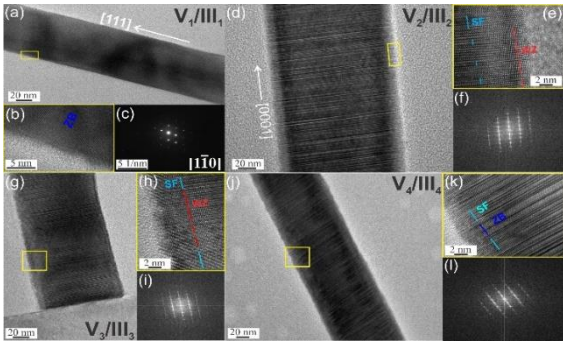


Fig. 2. HRTEM Morphology of InAs SAG for different molar flow. (a), (d), (g) and (j) are low magnification view of samples  $V_1/\text{III}_1$  to  $V_4/\text{III}_4$ . (b), (e), (h) and (k) are high magnification view of samples  $V_1/\text{III}_1$  to  $V_4/\text{III}_4$ . Blue, red and light blue lines represent ZB, WZ and SF segments, respectively. (c), (f), (i) and (l) SAD and FFT images of InAs NW.

TEM images of SAG-InAs NWs for different molar flows are shown in Fig. 2. Low, high magnification view and selective area diffraction (SAD) ( $[1\bar{1}0]$  zone axis) prove of that sample  $V_1/\text{III}_1$  exhibits pure ZB (blue line) crystal structure without any crystal phase mixture as shown in Fig. 2 (a) - (c). Sample  $V_2/\text{III}_2$  shows dominated WZ (red line) InAs with SF (light blue) crystal structure as shown in Fig. 2 (d) and (e). Supply of large  $V/\text{III}$  gas phase at constant growth temperature introduces kinetically limited InAs growth, whereas for low  $V/\text{III}$  supply, the NW nucleation follows mass transport and temperature dependent growth (complete TMI decomposition). As a consequence, In rich environment at large  $V/\text{III}$  gas phase forms WZ dominated crystal structure from virtual low temperature region [6]. However, SFs still persists in the NWs which is shown in Fig. 2 (f) fast Fourier transform image (FFT). Further reduction in molar flow results in the increase of SF by significantly decreasing WZ segment as shown in Fig. 2 (g), (h), (j) and (k). Double diffraction point with streaky line from Fig. 2 (i) and (l) confirms the influence of SF and polytype on SAG-InAs NW crystal structure. Raman spectrum shown in Fig. 3 (a) was measured on as-grown SAG-InAs NW samples for different molar ratio. There are two peaks observed in Raman spectra, strong transverse-optical (TO) phonon spectra ( $\sim 212$ - $218$   $\text{cm}^{-1}$ ) with weak longitudinal-optical (LO) ( $238$ - $240$   $\text{cm}^{-1}$ ) spectra. To find the possibility of WZ and ZB presence, spectra is deconvoluted with Lorentz fit. Upon deconvolution, lower and higher frequency was observed around  $211$ - $214$   $\text{cm}^{-1}$  (WZ) and  $215$ - $217$   $\text{cm}^{-1}$  (ZB), respectively.

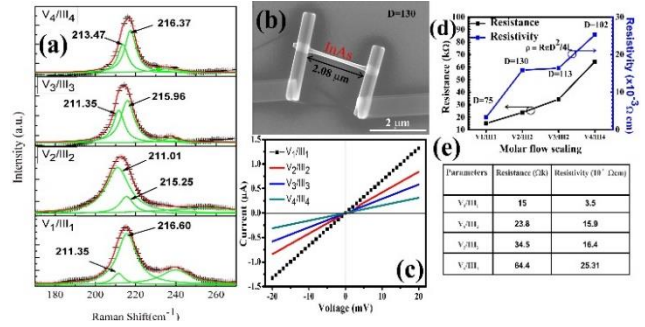


Fig. 3. (a) Raman spectrum of as-grown SAG-InAs NWs for different molar flow. Cumulative fit (red), extracted data (+) and their Lorentz fit (red). (b) SEM image of a single InAs NW device. (c), (d) and (e) are I-V characteristics and variation of resistance, resistivity for the NWs with different molar flow rate.

To investigate electrical performance, the resistance of those NWs were calculated from I-V curves as shown in Fig. 3 (b). Here resistivity of pure ZB NWs ( $V_1/\text{III}_1$ ) calculated to be  $3.5 \times 10^{-3} \Omega \text{cm}$  (15 k $\Omega$ ), which is significantly low, compared to other undoped NW reports. This low resistivity may attributes to an unintentional carbon incorporation at high molar flow and low growth temperature. When the WZ and SF incorporate into NWs, resistivity of the NWs strongly increases. Obtained resistivity (resistance) of samples are shown in fig. 3 (e). A strong discontinuity in conduction band (30-90 meV) between InAs WZ to InAs ZB crystal structure, causes an increase in resistivity of several orders [7].

#### 4. Conclusion

In this study, the change in crystallographic structure and electrical characteristics of the SAG-InAs NW were studied. It was shown that when the selectivity increases with the reduction of molar flow rate, the WZ dominated InAs NW nucleation was observed under kinetically limited growth region. Further scaling down the molar flow results in equally mixed WZ/ZB crystal structure. Meanwhile, WZ dominated SAG-InAs NW ( $15.9 \times 10^{-3} \Omega \text{cm}$ ) gives resistivity value 1.6 times lower than equally mixed InAs NW ( $25.31 \times 10^{-3} \Omega \text{cm}$ ).

#### Acknowledgements

This work was sponsored by the TSMC, NCTU-UCB I-RiCE program, and Ministry of Science and Technology, Taiwan, under Grant No. MOST 106-2911-I-009-301.

#### References

- [1] M.G. Lagally and R.H. Blick, Nature **432** (2004) 450.
- [2] K. Tomioka, J. Motohisa, S. Hara, and T. Fukui, Jpn. J. Appl. Phys. **46** (2007) 1102.
- [3] B. Feng, S. Huang, J. Wang, D. Pan, J. Zhao, and H. Q. Xu, J. Appl. Phys. **119** (2016) 054304.
- [4] A. Fontcuberta i Morral, C. Colombo, G. Abstreiter, J. Arbiol, and J. R. Morante, Appl. Phys. Lett. **92** (2008) 063112.
- [5] X. Wang, W. Yang, B. Wang, X. Ji, S. Xu, W. Wang, and T. Yang, J. Cryst. Growth **460** (2017) 1.
- [6] S. Lehmann, D. Jacobsson, and K. A. Dick, Nanotechnology, **26** (2015) 301001.
- [7] C. Thelander, P. Caroff, S. Plissard, A. W. Dey and K. A. Dick, Nano Lett. **11** (2011) 2424.